Neuron, Vol. 33, 39–50, July 3, 2002, Copyright ©2002 by Cell Press

Drosophila Homeodomain Protein dHb9 Directs Neuronal Fate via Crossrepressive and Cell-Nonautonomous Mechanisms

Heather T. Broihier and James B. Skeath[1]
Department of Genetics
Washington University School of Medicine
St. Louis, Missouri 63110

Summary

Here we present the identification and characterization of *dHb9*, the *Drosophila* homolog of vertebrate *Hb9*, which encodes a factor central to motorneuron (MN) development. We show that dHb9 regulates neuronal fate by restricting expression of Lim3 and Even-skipped (Eve), two homeodomain (HD) proteins required for development of distinct neuronal classes. Also, dHb9 and Lim3 are activated independently of each other in a virtually identical population of ventrally and laterally projecting MNs. Surprisingly, dHb9 represses Lim3 cell nonautonomously in a subset of dorsally projecting MNs, revealing a novel role for intercellular signaling in the establishment of neuronal fate in *Drosophila*. Lastly, we provide evidence that dHb9 and Eve regulate each other's expression through Groucho-dependent crossrepression. This mutually antagonistic relationship bears similarity to the crossrepressive relationships between pairs of HD proteins that pattern the vertebrate neural tube.

Introduction

The generation of individual neuronal fates in the embryo is fundamental to mature CNS function. While proper cell fate specification is of obvious importance in all developing tissues, it is particularly critical in CNS development due to the tremendous diversity of CNS cell types and the fact that neuronal fates are assigned at the level of the single cell. Though unique, individual neurons can be grouped together based on shared characteristics such as axonal trajectory or neurotransmitter expression. Work from vertebrates and invertebrates has demonstrated that these common neuronal properties are often coordinately regulated at the molecular level (see Jessell, 2000), a mechanism that clearly simplifies the task of specifying a great diversity of functional neurons.

In *Drosophila*, roughly 400 neurons are generated from 30 neuroblasts (NBs) in each hemisegment of the embryonic CNS (Schmid et al., 1999). Each NB lineage arises via rounds of stem cell division that produce secondary precursor cells called ganglion mother cells (GMCs), which divide asymmetrically to produce two postmitotic neurons or glia. While each lineage is unique, all lineages give rise to multiple neuronal types, and moreover, functional classes of neurons are distributed widely across NB lineages. For example, the 32 motorneurons (MNs) specified in each abdominal hemisegment arise from roughly half the 30 NB lineages (Bossing et al., 1996; Schmid et al., 1999). Since each NB produces a largely invariant clone of neurons, it has been proposed that neuronal fate is directed in a lineage-intrinsic manner via factors inherited from the parental NB (Huff et al., 1989). Cell interactions between neurons of different lineages are not thought to regulate neuronal fate.

Several conserved homeodomain (HD) proteins have been shown to govern neuronal identities. In particular, LIM-HD proteins are critical for neuronal fate determination and axonal pathfinding. These proteins direct cell fates in a combinatorial manner, such that a neuron's fate depends on the particular combination of LIM-HD proteins it expresses. This model originated from work in vertebrates demonstrating that classes of MNs with distinct axonal trajectories express unique combinations of LIM-HD proteins (Appel et al., 1995; Tsuchida et al., 1994). Subsequently, loss-of-function and misexpression experiments in *Drosophila* and vertebrates suggested that axonal outgrowth can be predictably altered by changing the complement of LIM-HD proteins expressed in particular groups of MNs (Sharma et al., 1998; Thor and Thomas, 1997; Thor et al., 1999). Similarly, the evolutionarily conserved Evx/Eve HD transcription factors play essential roles in neuronal determination. The mouse Eve homolog, Evx1, is expressed in a specific class of interneurons, and *evx1* mutant mice display cell fate transformations consistent with a role for Evx1 as a determinant of interneuron fate (Moran-Rivard et al., 2001). In *Drosophila*, Eve is expressed in MNs that innervate dorsal muscle targets, and its expression in MNs is necessary and sufficient to direct motor axons to the dorsal muscle field (Doe et al., 1988; Landgraf et al., 1999). Despite the identification of a handful of genes that regulate neuronal fate, the genetic regulatory network within which these genes function remains largely undefined.

The related vertebrate HD proteins, Hb9 and MNR2, are additional elements of the transcriptional code that defines distinct neuronal identities (Arber et al., 1999; Saha et al., 1997; Tanabe et al., 1998; Thaler et al., 1999). In chick, MNR2 is expressed only by MN progenitors, and Hb9 only by postmitotic MNs. In mice, there does not appear to be an MNR2 homolog, and Hb9 is expressed in both MN progenitors and postmitotic MNs. Functional studies indicate that these proteins distinguish MN and interneuron identities. Misexpression of either protein in the chick neural tube transforms interneurons to MNs (Tanabe et al., 1998). Conversely, in *Hb9* mutant mice, MNs are still generated, though they inappropriately express several interneuron-specific genes (Arber et al., 1999; Thaler et al., 1999). Thus, Hb9 is thought to contribute to MN fate by repressing interneuron-specific gene expression within MNs. This work clearly underlines the importance of Hb9 in MN development. Yet the mechanisms through which the nervous system integrates Hb9 function with that of other neuronal fate determinants are largely unknown.

In this paper, we present the identification and characterization of *Drosophila Hb9*. We address the relation-

[1] Correspondence: jskeath@genetics.wustl.edu

ship of dHb9 to three HD proteins known to govern neuronal identity—Islet, Lim3, and Eve. Our data shed light on the mechanisms regulating the specific combinatorial expression of these factors. We find that dHb9 and Lim3 are activated independently of each other in virtually identical patterns of ventrally and laterally projecting MNs. We also present evidence that dHb9 acts cell nonautonomously to repress Lim3 expression in a subset of dorsally projecting MNs. This result reveals a novel role for intercellular signaling in neuronal fate determination. In addition, genetic studies demonstrate that dHb9 and the dorsal MN determinant Eve engage in a crossinhibitory interaction to help distinguish distinct neuronal classes. Taken together, our work establishes dHb9 as a key component of the combinatorial code that defines neuronal fates and elucidates the genetic regulatory network through which dHb9, Lim3, Islet, and Eve control neuronal identity.

Results

Eve Is Derepressed in *exex* Mutant Embryos

To identify genes required for proper neuronal fate specification in the *Drosophila* embryonic CNS, we conducted an EMS saturation mutagenesis of the third chromosome and screened for changes in the CNS expression pattern of Eve (J.B.S. and C.Q. Doe, unpublished data). We assayed for changes in Eve expression because Eve is expressed in a stereotyped pattern of eight dorsally projecting MNs and 12 interneurons in each abdominal hemisegment (Figure 1A; Patel et al., 1989), and because *eve* is a known regulator of neuronal fate (Landgraf et al., 1999).

We identified four alleles of one locus we called *extra-extra* (*exex*). *exex* mutant embryos display a highly specific phenotype in which two ectopic Eve-expressing neurons develop per hemisegment (Figure 1B). These ectopic Eve-positive neurons appear during late stage 11 in the vicinity of the Eve-positive neurons aCC/pCC (brackets in Figures 1A and 1B). By stage 14, one ectopic Eve-expressing neuron is found adjacent to aCC/pCC (open arrowheads in Figure 1B), while the other migrates posteriorly and laterally (closed arrowheads in Figure 1B) to adopt a stereotyped mediolateral position.

To examine more closely the cell fate changes that occur in *exex* mutant embryos, we set out to determine the lineal origin of the ectopic Eve-positive neurons. Since in *exex* mutants, the ectopic Eve-expressing neurons arise immediately adjacent to the sibling aCC/pCC neurons, we hypothesized that, like aCC/pCC, the ectopic Eve-positive neurons derive from the NB1-1 lineage. To test this, we assayed whether an Eve-β-gal reporter gene normally expressed solely by the aCC/pCC and RP2 neurons (Fujioka et al., 1999) is also expressed by the ectopic Eve-positive neurons in *exex* mutant embryos. In support of our model, both ectopic Eve-positive neurons express β-gal in *exex* mutant embryos (arrowheads in Figure 1C), indicating that the ectopic Eve-positive neurons likely arise within the NB1-1 lineage. These date indicate that *exex* regulates neuronal fate by repressing *eve* expression in the NB1-1 lineage.

exex Corresponds to *Drosophila Hb9*

The ability of *exex* to regulate neuronal fate by repressing *eve* places *exex* within the genetic regulatory network that governs neuronal fate. To begin to illuminate the role *exex* plays in this network, we characterized *exex* at the molecular level. Standard meiotic mapping positioned *exex* between *ru* and *h* on the genetic map, and deficiency analysis localized *exex* to cytological position 66B1-2. The subsequent completion of sequencing of the *Drosophila* genome facilitated a candidate gene approach to identify *exex*. We screened predicted genes in the region for a CNS expression pattern by RNA in situ hybridization, and identified one gene, *CG8254*, expressed in the embryonic CNS (data not shown). To determine if this gene corresponds to *exex*, we sequenced the *CG8254* coding region from larvae homozygous for each *exex* allele. We found that each *exex* allele contains a distinct nonsense mutation in the *CG8254* coding region (Figure 1D). These data and our finding that $exex^{KK30}$ homozygous mutant embryos fail to produce detectable Exex protein (Figure 2D) demonstrate that the *exex* locus corresponds to *CG8254*.

Comparative sequence analysis indicates *exex* codes for the *Drosophila* homolog of the vertebrate HD proteins MNR2/Hb9 (Figure 1E). Within the HD, Exex is 90% identical and 95% similar to MNR2/Hb9. The next most closely related *Drosophila* HD protein, Deformed, shares only 68% identity with Hb9/MNR2, indicating that *exex* is the sole Hb9/MNR2 homolog in *Drosophila*. Therefore, from this point on, we refer to *exex* as *dHb9*. Outside the HD, the largest region of homology between dHb9 and Hb9 bears some sequence similarity to the TN domain of Nkx and Dbx class HD proteins (Figure 1F). The TN domain has been shown to mediate the repressive ability of these proteins and to interact with the Groucho corepressor (Jiménez et al., 1997; Muhr et al., 2001). These data and the requirement of *dHb9* to repress *eve* suggest dHb9 functions as a transcriptional repressor during CNS development.

dHb9 Is Expressed in a Subset of Motorneurons and Interneurons

To investigate the role of dHb9 during CNS development, we raised dHb9-specific antibodies. Embryonic expression of dHb9 initiates in the posterior midgut primordium at stage 7 (data not shown). By stage 9, dHb9 protein is present in the primordia of the anterior and posterior midgut (Figure 2A) and persists in anterior and posterior regions of the endoderm throughout embryogenesis (data not shown). In the CNS, we first detect dHb9 protein expression during stage 11 in one-to-two mitotic GMCs and approximately 15 neurons per hemisegment (Figure 2B). dHb9 expression in the CNS peaks at stage 14,when it is strongly expressed in approximately 30 neurons per hemisegment, including the well-characterized RP1, RP3-5 MNs, and dMP2 and MP1 interneurons (Figure 2C; Figures 4B and 4E) . Thus, in the CNS, dHb9 expression is expressed almost exclusively in a distinct population of postmitotic MNs and interneurons, consistent with dHb9 regulating neuronal identity.

To verify the specificity of the dHb9 antibodies, we examined dHb9 expression in embryos homozygous for

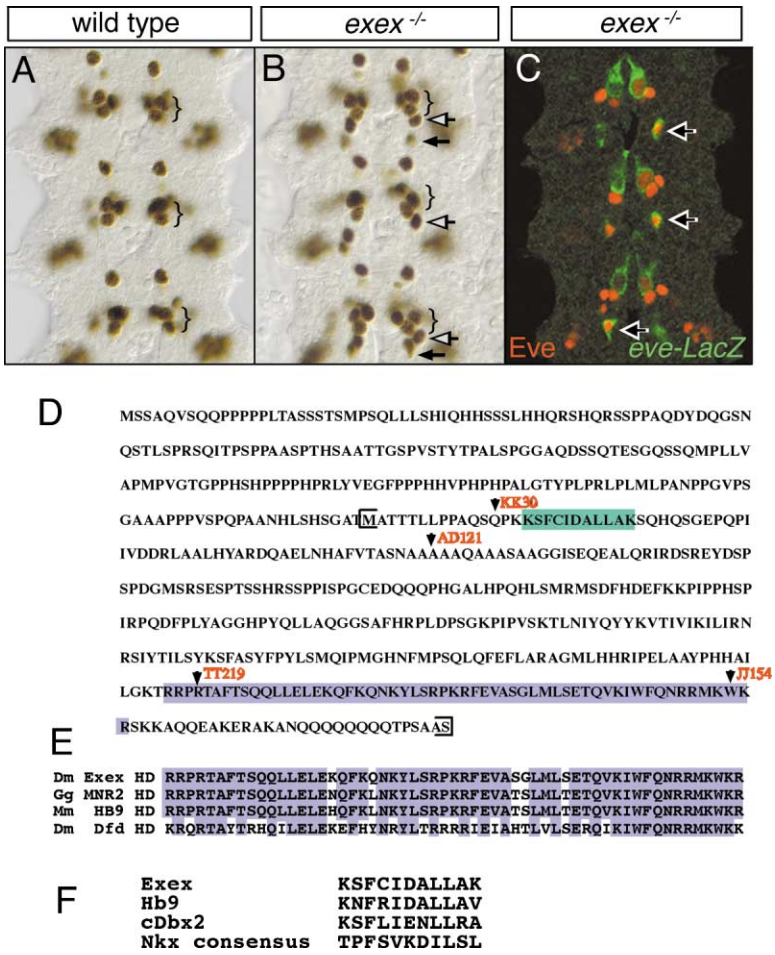

Figure 1. *exex* Corresponds to the *Drosophila* Hb9/MNR2 Homolog

(A) Stage 14 wild-type and (B) *dHb9*^{KK30} homozygous embryos stained with Eve. On average, two ectopic Eve-positive cells arise in *dHb9* mutants (B). One remains immediately posterior to aCC/pCC (open arrows); the other migrates posteriorly (closed arrows). (C) *dHb9*^{KK30} embryo carrying an *eve-LacZ* reporter expressed in aCC/pCC and RP2 double stained for Eve and β-gal. The ectopic Eve-positive neurons express β-gal, consistent with them arising from the NB1-1 lineage. This focal plane shows only the posteriorly migrating neuron (open arrows). (D) dHb9 protein sequence with putative TN domain in green, HD in blue, and positions of the four nonsense codons shown in red. Region of dHb9 included in the protein expression construct is bracketed. (E) Alignment of the dHb9, MNR2, Hb9, and Dfd HDs. (F) Alignment of the putative TN domains of dHb9 and Hb9 with Dbx2 TN domain and the consensus Nkx TN domain.

each dHb9 allele. Confirming antibody specificity, we fail to detect dHb9 protein in embryos homozygous for the most 5′ nonsense mutation, *dHb9*^{KK30} (Figure 2D). In addition, these data and the identical phenotypes of *dHb9*^{KK30} homozygous and *dHb9*^{KK30}*/Df(pbINR)* transheterozygous embryos (data not shown) identify *dHb9*^{KK30} as a null allele. Interestingly, dHb9 protein is present at wild-type levels in embryos homozygous for *dHb9*^{JJ154}, an allele predicted to encode the entire protein except the C-terminal 32 amino acids (Figure 1D). Since *dHb9*^{JJ154} embryos exhibit similar, albeit more severe, CNS phenotypes than *dHb9*^{KK30}embryos, the *dHb9*^{JJ154} allele likely has dominant-negative activity.

dHb9 MNs Populate the Majority of Motor Axon Branches

A key distinguishing trait of neurons is their axonal trajectory. Thus, we wanted to trace the axonal trajectories of dHb9-positive neurons to investigate whether dHb9 identifies specific subpopulations of CNS neurons. To create a dHb9-dependent axonal marker, we employed targeted transposition to convert a *dHb9*^{LacZ} enhancer trap to a *dHb9*^{Gal4} enhancer trap (Experimental Procedures; Sepp and Auld, 1999). We used the *dHb9*^{Gal4} driver to express GAP-GFP and confirmed that GFP expression faithfully recapitulates the dHb9 expression pattern (Figure 2F) with the exception that the peripheral LBD neuron expresses *dHb9*^{Gal4} but not dHb9 (LBD in Figures 2G–2H). Within the CNS, we find that dHb9-positive interneurons project axons in three distinct longitudinal fascicles (data not shown).

We next traced the trajectory of dHb9-positive MNs into the periphery and found that dHb9-positive neurons populate five of the six motor axon branches. In *Drosophila,* motor axons exit the CNS in the ISN, SN, and transverse nerve (TN). The main branch of the ISN innervates the dorsal and lateral body wall musculature. Axons in two branches of the ISN, ISNb, and ISNd defasciculate from the ISN to innervate distinct groups of ventral body wall muscles. Similarly, the primary branch of the SN, SNa, innervates a lateral muscle group, and axons in its minor branch, SNc, extend along SNa until their choice point where they defasciculate and innervate ventral muscles. We find that dHb9-positive motor axons extend in the ISN, ISNb, ISNd, Sna, and SNc nerves (Figures 2G and 2H). While we observe dHb9-positive motor axons in the ISN, they do not project to the most dorsal muscle regions (arrows in Figure 2H and see below). In addition, we fail to detect dHb9-positive axons in the TN. These data demonstrate that dHb9-positive axons populate five of the six major nerve branches and that dHb9 is expressed in the majority of ventrally and laterally projecting MNs. Interestingly, dorsally projecting MNs express Eve (Landgraf et al., 1997, 1999;

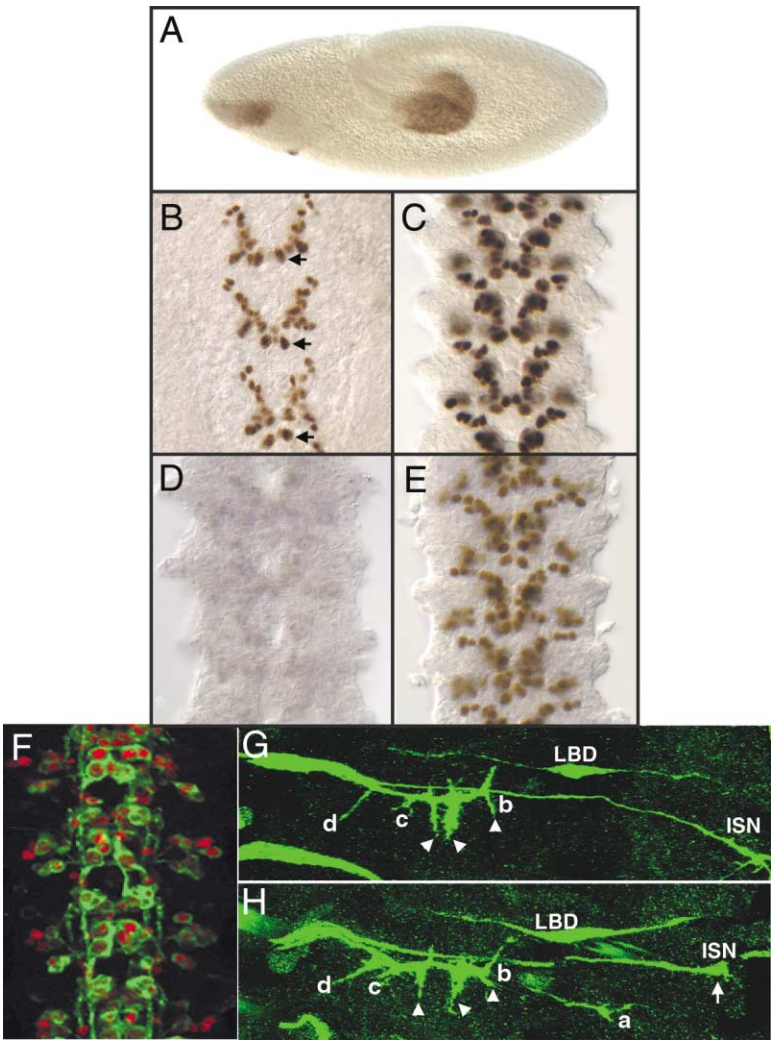

Figure 2. dHb9 Is Expressed in Motorneuron and Interneuron Subsets

(A) Stage 9, (B) stage 11, (C) stage 14 wild-type embryos as well as stage 14 (D) *dHb9*^{KK30} and (E) *dHb9*^{JJ154} homozygous embryos stained for dHb9. (A) dHb9 is expressed in the anterior and posterior midgut invaginations. (B) dHb9 is expressed in roughly 15 neurons/hemisegments at stage 11, dMP2 is indicated by arrows. (C) dHb9 is expressed in about 30 neurons/hemisegments by stage 14. (D) *dHb9*^{KK30} embryo lacks virtually all dHb9 protein expression while (E) *dHb9*^{JJ154} embryos display wild-type dHb9 levels. (F–H) Stage 16 *dHb9*^{Gal4}*/UAS-GAPGFP* embryos stained with dHb9 (red) and GFP (green). (F) *dHb9*^{Gal4} is expressed in all dHb9-positive neurons. The only difference we detect between dHb9 and *dHb9*^{Gal4} expression is that *dHb9*^{Gal4} is expressed in the peripheral LBD neuron while dHb9 is not. (G–H) dHb9 is expressed in the main ISN branch, ISNb (arrowheads), ISNd, SNa, and SNc.

Schmid et al., 1999), but apparently not dHb9, suggesting that dHb9 and Eve identify distinct populations of MNs (see below).

dHb9 Is Required for Motorneuron Pathfinding

The widespread expression of dHb9 in MNs led us to ask whether *dHb9* regulates MN differentiation. To address this, we used MAb 1D4 against Fasciclin II (Van Vactor et al., 1993) to visualize MN projections in embryos mutant for the null allele, *dHb9*^{KK30}. The overall organization of motor axon projections is normal, and we do not detect pathfinding aberrations in either SN branch or in the ISN or ISNd. However, the ISNb branch exhibits two predominant phenotypes both resulting in a lack of innervation of the ventral muscle field. In 41% of hemisegments (n = 188), the ISNb defasciculates from the ISN and enters the ventral musculature, where the axons stall and growth cones accumulate (arrows in Figure 3B). In 19% of hemisegments, the ISNb fails to defasciculate from the ISN and extends dorsally with the ISN (anterior two hemisegments in Figure 3C). Since dHb9 is expressed in the ISNb-projecting RP MNs, the aberrant pathfinding of ISNb in *dHb9* mutants suggests that *dHb9* promotes the differentiation of these neurons.

Our loss-of-function analysis indicates that *dHb9* is necessary for the proper axonal trajectories of a subset of ventrally projecting MNs. To test whether dHb9 misexpression is sufficient to reroute motor axons, we misexpressed dHb9 via the UAS/Gal4 system (Brand and Perrimon, 1993). Embryos in which we misexpress dHb9 in all postmitotic neurons via the elavGal4 driver display highly penetrant axonal phenotypes (Figure 3D). In these embryos, all motor axons fuse with the ISN prior to exiting the CNS. Thus, only a single nerve branch, a thickened ISN, forms in these embryos. The thickness of the ISN decreases dramatically in the lateral muscle region, suggesting that most axons acquire a laterally projecting ISN identity. Consistent with this, the ISN terminates prematurely in the dorsal body wall and often branches aberrantly in this region (Figure 3D). The defects in dorsal MN projections likely arise as a result of the ability of dHb9 misexpression to abolish Eve in dorsally projecting MNs (see below and Discussion). We conclude dHb9 misexpression forces MNs to acquire an ISN-projecting identity and preferentially induces these MNs to project to the lateral body wall region. In combination with the loss-of-function analysis, these data demonstrate that proper levels of dHb9 activity are re-

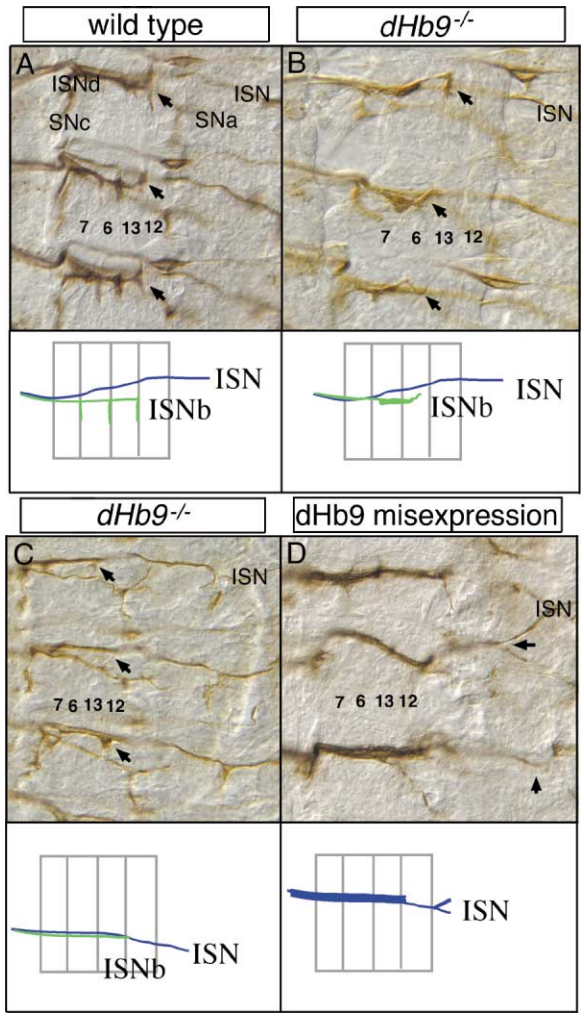

Figure 3. *dHb9* Is Required for Motor Axon Projections

(A–D) Dissected stage 17 embryos stained with anti-FasII antibody. Positions of the ventral muscles (7, 6, 13, 12) are indicated in each panel. Arrows point to ISNb in (A)–(C). Schematics of the wild-type or mutant projection patterns are shown below each figure. (A) In wild-type, ISNb innervates ventral muscles 7, 6, 13, and 12 in a stereotyped pattern (arrows). The positions of the other nerve branches are indicated. In $dHb9^{KK30}$ embryos, the ISNb projects aberrantly after defasciculating from the ISN (B), or fails to defasciculate from the ISN (anterior 2 hemisegments in [C]). (D) In *elavGal4/UAS-dHb9* embryos, all motor axons fuse with the ISN. Dorsally, the ISN truncates prematurely (arrow in posterior hemisegments) or branches aberrantly (arrow in middle hemisegment).

quired to direct the normal pattern of motor axon outgrowth.

dHb9 Is Coexpressed with Lim3 and Islet

The ISNb MN phenotypes of dHb9 exhibit similarity to those of Lim3 and Islet. Lim3 and Islet are two LIM-HD proteins that are required for the development of ISNb-projecting axons (Thor and Thomas, 1997; Thor et al., 1999). As noted, ISNb-MNs express dHb9 and require dHb9 function for their differentiation, suggesting that dHb9 might interact with Lim3 and Islet to regulate neuronal fate. To investigate this, we assayed the relative expression patterns and genetic interactions between these genes. To this end, we first generated Lim3- and Islet-specific antibodies because prior expression analyses of Lim3 and Islet used gene-specific reporter constructs (Thor and Thomas, 1997; Thor et al., 1999) and such reporter constructs often identify only a subset of a gene's expression profile.

We find that Lim3 is expressed in about 40 neurons per hemisegment (Figure 4A)—many more neurons than previously identified by reporter gene expression. Of particular interest, Lim3 is expressed in all dHb9-positive neurons (Figure 4B) as well as in several lateral dHb9-negative neurons, including the Eve-positive EL interneurons (closed arrowheads in Figures 4B and 4C). Therefore, like dHb9, Lim3 is expressed in MNs projecting in the primary and secondary branches of both the SN and ISN. Since previous work has demonstrated that Lim3 is expressed in the TN nerve (Thor et al., 1999), we conclude that Lim3 is expressed in all motor axon branches and suggest that all ventrally and laterally projecting MNs may express Lim3.

Despite the near identity of the dHb9 and Lim3 expression patterns, dHb9 and Lim3 do not activate each other's expression in these cells. dHb9 expression initiates normally in *lim3* mutants and Lim3 expression in dHb9-expressing cells also initiates normally in *dHb9* mutants (data not shown). These data demonstrate that dHb9 and Lim3 are activated independently of each other in coexpressing cells and suggest that they act in parallel to specify neuronal identity. In addition, the striking similarity of the dHb9 and Lim3 expression patterns suggests coregulation of Lim3 and dHb9 by a largely overlapping set of transcriptional regulators.

We find more limited overlap in the expression patterns of dHb9 and Islet. Islet is expressed in roughly 30 neurons per hemisegment (Figure 4D), the majority of which are located laterally in the CNS. dHb9 and Islet are coexpressed in three discrete neuronal populations (Figure 4E): the medial ISNb-projecting RP MNs (open arrowheads in Figure 4E), a pair of mediolateral interneurons corresponding to the serotonergic interneurons of the CNS (closed arrowheads in Figure 4E; Lundell and Hirsch, 1994; Thor and Thomas, 1997), and a compact cluster of six lateral neurons (arrows in Figure 4E). As observed for dHb9 and Lim3, dHb9 and Islet do not regulate each other's expression—Islet expression is normal in *dHb9* mutant embryos and dHb9 expression is normal in *isl* mutant embryos (data not shown). These results indicate that *dHb9* and *isl* do not fall into a simple linear hierarchy and suggest they act in parallel to specify neuronal fate.

Coordinate Regulation of Axonal Pathfinding by dHb9 and Islet

To investigate whether *dHb9* and *Islet* act in parallel, we constructed *isl; dHb9* double mutants and analyzed axonal organization in these embryos. *isl* or *dHb9* single mutant embryos exhibit no overt defects in the overall architecture of the CNS (data not shown). In contrast, *isl; dHb9* double mutant embryos exhibit clear defects in the organization of the axonal scaffold (Figures 5A and 5B). For example, the anterior and posterior commissures are thinner than in wild-type and frequently only one commissure forms per segment. In addition,

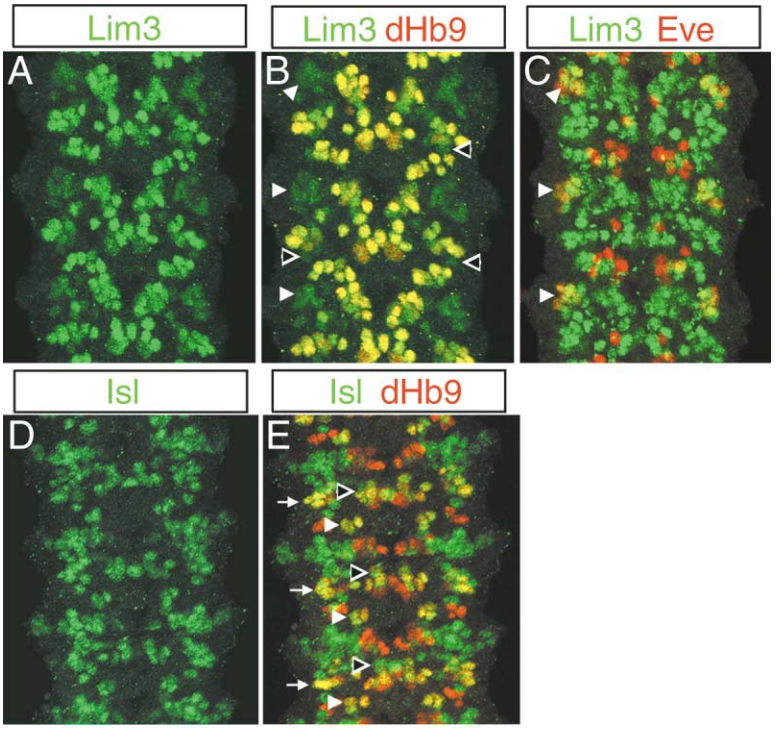

Figure 4. dHb9 Is Coexpressed with Lim3 and Islet

(A–E) Wild-type stage 14 embryos labeled with indicated antibodies. (A) Lim3 is expressed in roughly 40 neurons per hemisegment. (B) dHb9 (red) is expressed in a subset of Lim3-expressing neurons (green). Lim3 is also expressed in lateral dHb9-negative neurons (open and closed arrowheads in [B]–[C]). (C) Eve (red) and Lim3 (green) are coexpressed in the lateral EL interneurons (closed arrowheads). (D) Islet is expressed in about 30 neurons per hemisegment. (E) dHb9 (red) and Isl (green) are coexpressed in three neuronal groups: the medial RP MNs (open arrowheads); the paired serotonergic interneurons (closed arrowheads); and a lateral cluster of six neurons (arrows).

the longitudinal connectives are thinner than in wild-type and often veer toward or away from the midline.

The defects in axonal organization in *isl; dHb9* double mutants suggested these embryos might exhibit pronounced defects in motor axon projections. Whereas the axonal phenotypes of both single mutants are confined to the ISNb nerve branch (Figures 3B and 3C; Thor and Thomas, 1997), double mutant embryos display widespread defects (Figures 5C–5E). In *isl; dHb9* double mutants, the organization of motor axons into five nerve branches usually occurs, though axonal outgrowth is substantially delayed relative to wild-type. In addition, the penetrance of ISNb phenotypes in *isl; dHb9* double mutant embryos is dramatically higher than in *dHb9* single mutants (arrows in Figure 5C). In 96% of hemisegments (n = 86), the ISNb either bypasses the ventral muscle domain and extends along the ISN, or stalls shortly after it defasciculates from the ISN. Furthermore, we observe defects in the main ISN branch. In 32% of hemisegments (n = 86), ISN axons defasciculate inappropriately, giving the ISN a "frayed" appearance (arrows in Figure 5D). At lower frequency (5%), the ISNs from adjacent hemisegments fuse (arrows in Figure 5E). The ISN phenotypes are consistent with the presence of dHb9-positive axons in the ISN and demonstrate that like ISNb, the ISN is sensitive to *dHb9* levels. Since it is unclear whether Isl is expressed in ISN-projecting neurons, the ISN phenotype in *isl; dHb9* embryos may result from loss of *isl* and *dHb9* activity either in common or distinct neuronal populations. In conclusion, the widespread axonal phenotypes in *isl; dHb9* double mutant embryos indicate that *isl* and *dHb9* act in parallel to regulate neuronal differentiation. Furthermore, the fact that the *isl; dHb9* double mutant reveals a role for *dHb9* in regulating ISN-projecting axons suggests that *dHb9* may genetically interact with other factors to control the outgrowth of additional motor axon branches.

dHb9 Represses Eve

Our expression analyses indicate that dHb9 and Lim3 are expressed widely in ventrally and laterally projecting MNs. In contrast, Eve has been shown to be expressed in dorsally projecting MNs (Landgraf et al., 1999), suggesting that dHb9/Lim3 and Eve might label nonoverlapping MN populations. This is, in fact, what we observe as dHb9 and Eve label mutually exclusive neuronal subsets (Figures 6A and 6B). Lim3 and Eve also identify nonoverlapping sets of MNs, since they are only coexpressed in the EL interneurons (Figure 4C). Together with our other expression analyses, these data show that dHb9/Lim3 are expressed in the majority of Eve-negative MNs and demonstrate that dHb9/Lim3 and Eve identify distinct MN classes.

As described above, *dHb9* mutant embryos display several ectopic Eve-positive neurons (Figures 1A and 1B). Using the protein-positive *dHb9*^{JJ154} allele (Figure 1E), we find that these ectopic Eve cells arise from cells that normally express dHb9 (data not shown), suggesting that dHb9 represses Eve cell autonomously. The nonoverlapping expression patterns of dHb9 and Eve further indicate that dHb9 acts operationally as an Eve repressor in the CNS. To investigate whether dHb9 is sufficient to repress Eve, we misexpressed dHb9 in all postmitotic neurons and find that dHb9 represses Eve in all Eve-positive neurons except the EL neurons (compare Figures 6C and 6D). By late stage 14, only one or two weakly Eve-positive neurons remain in the positions normally occupied by the U, RP2, a/pCC, and fpCC neurons, while the cluster of Eve-positive EL interneurons appears normal (arrows in Figure 6D). Thus, dHb9

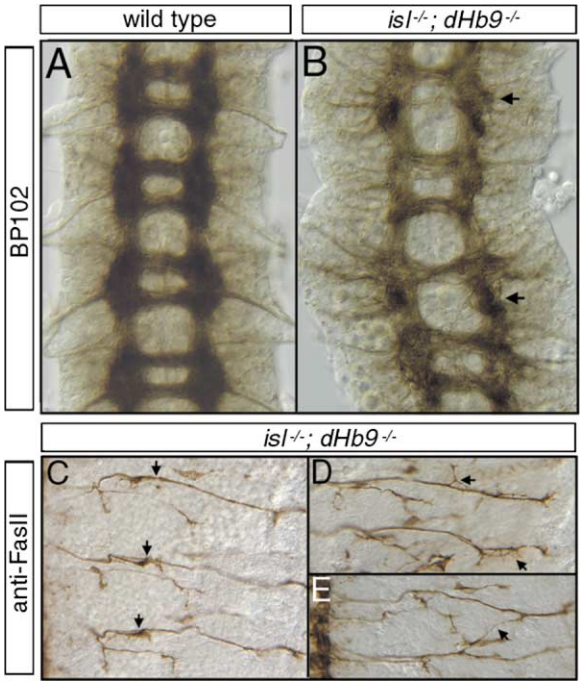

Figure 5. *dHb9* and *isl* Act in Parallel to Promote Proper Axonal Pathfinding

(A) Stage 16 wild-type and (B) *isl; dHb9* double mutant embryos stained with BP102. The scaffold of CNS axons is aberrant in *isl; dHb9* double mutants, and the commissures are often greatly reduced or absent (arrows in [B]). (C–E) *isl; dHb9* double mutant embryos stained with anti-FasII. Compare to wild-type embryo in Figure 4A. ISNb projections clump in the proximity of the ISN (arrows in [C]). Axons within the ISN defasciculate aberrantly (arrows in [D]). (E) ISNs from adjacent hemisegments also fuse across the parasegment boundary (arrows).

expression is sufficient to repress Eve expression in all dorsally projecting MNs. The inability of dHb9 to repress Eve expression in the ELs suggests that the relative ability of dHb9 to repress Eve is controlled by factors expressed specifically in different neuronal types.

Eve Represses dHb9 in a Groucho-Dependent Fashion

The mutually exclusive expression patterns of Eve and dHb9 and the ability of dHb9 to repress Eve led us to investigate whether Eve exhibits a reciprocal ability to repress dHb9. We tested whether *eve* represses *dHb9* by following dHb9 in eve^{1D} mutant embryos. This temperature-sensitive allele allowed us to circumvent the early requirement for *eve* during embryonic segmentation (Experimental Procedures). On average, we observe two ectopic dHb9-positive neurons in each hemisegment of *eve* mutant embryos (Figure 6E). The position of these neurons identifies one as RP2 and the other as likely aCC or pCC. Therefore, *eve* exhibits a reciprocal ability to repress *dHb9* in a subset of dorsally projecting MNs.

During segmentation, Eve has been shown to act as a transcriptional repressor and contains two domains with repressive capability—one dependent on the corepressor Groucho (Gro) and one Gro independent (Jiménez et al., 1997; Kobayashi et al., 2001). To determine

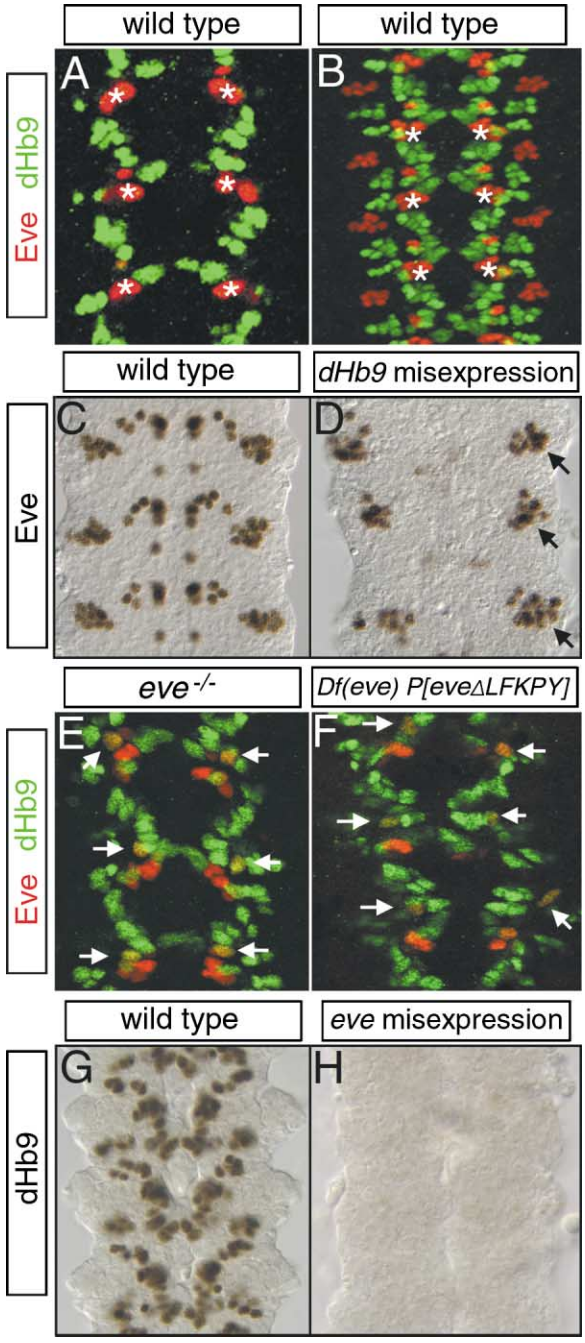

Figure 6. dHb9 and Eve Have Nonoverlapping Expression Patterns and Repress Each Other

(A) stage 12 and (B) stage 14 wild-type embryos. The expression of dHb9 (green) and Eve (red) is mutually exclusive. The U MNs are marked with (*) in (A)–(B). (C) wild-type and (D) *elavGal4/UAS-dHb9* mutant embryos labeled for Eve. dHb9 misexpression represses Eve in all neurons except the ELs (arrows in [D]). (E) Late stage 12 eve^{1D} and (F) *Df(eve) P{eveΔLFKPY}* mutant embryos labeled for Eve and dHb9. (E) dHb9 is derepressed in the RP2 MNs (arrows) as well as either aCC or pCC (posterior arrow in bottom left hemisegment). (F) dHb9 is similarly derepressed in RP2 (arrows) in *eve* mutants with a Gro-interaction domain deletion. (G) Wild-type and (H) *elavGal4/UAS-eve* mutant embryos labeled with DHb9. Eve misexpression abolishes dHb9 expression.

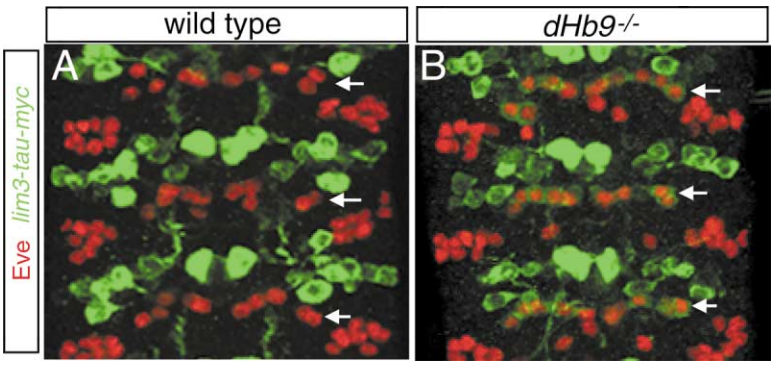

Figure 7. *dHb9* Represses *lim3* Cell Nonautonomously

Stage 15 (A) wild-type and (B) *dHb9*^{KK30} embryos carrying a *lim3-τmyc* reporter. (A) Lim3 is not expressed in the U MNs in wild-type, but is expressed in the U MNs in *dHb9* mutant embryos (B). Arrows indicate U MNs in both panels.

whether Eve requires Gro to repress dHb9 in the CNS, we assayed dHb9 expression in *eve* null embryos that contain an *eve* transgene deleted for the Gro-interaction domain (Kobayashi et al., 2001). In these embryos, dHb9 is derepressed in RP2 and one of the corner cells (Figure 6F). Since this phenotype is essentially identical to that of *eve*^{1D} mutants, we conclude that Eve represses dHb9 in a Gro-dependent manner. These results demonstrate that Eve/Evx proteins act through Gro to regulate cell fate in the CNS.

To investigate if Eve is also sufficient to repress dHb9, we misexpressed Eve in all postmitotic neurons. In these embryos, dHb9 expression is abolished (Figures 6G and 6H), demonstrating that Eve is a potent repressor of dHb9 expression in the CNS. Thus, Eve is both necessary and sufficient to repress dHb9. Taken together, our genetic studies demonstrate crossrepressive interactions between *dHb9* and *eve* function to delimit the expression of dHb9 to ventral and lateral MNs—and Eve to dorsal MNs. Since both dHb9 and Eve are key cell fate determinants, this mutually repressive relationship likely helps to consolidate distinct MN fates.

dHb9 Represses Lim3 Cell Nonautonomously

During our analysis of Lim3 expression in *dHb9* mutant embryos, we noticed the presence of a group of ectopic Lim3-positive neurons (Figure 7). Since all dHb9-positive neurons normally coexpress Lim3, the presence of ectopic Lim3-positive neurons suggests a cell-nonautonomous effect of dHb9 on the regulation of Lim3. Surprisingly, double label experiments identify the ectopic Lim3-positive neurons as the six Eve-positive U MNs (arrows in Figure 7). We illustrate this phenotype using a *lim3-tau-myc* transgene (Thor et al., 1999) due to the perdurance of transgene expression in U MNs relative to the more transient expression of endogenous Lim3 in these cells. We attribute the transient nature of Lim3 expression in the U MNs to the ability of Eve to repress Lim3 (data not shown).

The ectopic expression of Lim3 in the U MNs in *dHb9* mutants is exciting because neither the U MNs nor their progenitors ever express dHb9 (data not shown). These data further support our model that dHb9 acts cell nonautonomously to repress Lim3 expression in the U MNs. Consistent with this, several groups of dHb9-positive neurons surround the U MNs during their development (U MNs indicated by (*) in Figures 6A and 6B). One or more of these groups of dHb9-positive neurons likely serve as the source of the signal received by the U MNs. Taken together, these results uncover a novel role for intercellular signaling in the establishment of neuronal fate in *Drosophila*.

Discussion

Every NB lineage in the *Drosophila* CNS gives rise to multiple neuronal types; for example, both MNs and interneurons are generated in roughly half of the 30 NB lineages (Bossing et al., 1996; Schmid et al., 1999). The common lineage of distinct neuronal populations necessitates the tight spatiotemporal regulation of factors directing these different identities. The importance of lineage-specific factors in neuronal fate determination does not, however, preclude the possibility of invariant intercellular signaling between neurons of different lineages contributing to the resolution of unique neuronal identities. In fact, our data support a role for *dHb9* in the cell-autonomous and nonautonomous regulation of several factors required for the development of distinct neuronal fates. Here we discuss not only the role of *dHb9* in the combinatorial code, but also the diverse mechanisms of neuronal fate acquisition that this study highlights.

An Evolutionarily Conserved Mechanism of *Hb9* Function?

We identified *dHb9* in a screen for alterations in the pattern of Eve expression in the embryonic CNS (Figure 1). We cloned *dHb9* and found it codes for the *Drosophila* homolog of Hb9 and MNR2, two HD factors required for vertebrate MN development (Arber et al., 1999; Tanabe et al., 1998; Thaler et al., 1999). Hb9 expression in mouse is restricted to MNs whose axons exit from the ventral side of the neural tube (v-MNs) (Thaler et al., 1999). v-MNs and V2 interneurons arise from common progenitors characterized by coexpression of Lim3 and Gsh4 (Sharma et al., 1998). This shared lineage necessitates the presence of factors that differentiate v-MNs and V2 interneurons. *Hb9* activity contributes to the v-MN/V2 interneuron distinction, as V2 interneuron-specific gene expression is derepressed in *Hb9* mutant mice (Arber et al., 1999; Thaler et al., 1999). Interestingly, MNs whose axons emerge from the dorsal side of the neural tube (d-MNs) and arise from an MN-specific progenitor pool do not require Hb9 function (Thaler et al., 1999). The restriction of Hb9 expression to those MNs arising

from Lim3/Gsh4-positive progenitors suggests that Hb9 function is required only in MNs that need to actively suppress an alternate genetic program.

In *Drosophila*, many NBs produce both MNs and interneurons, suggesting a widespread requirement for factors that function to arbitrate between alternate genetic programs. Our data suggest that *dHb9* acts cell autonomously to repress Eve in neurons in the NB1-1 lineage, whereas *dHb9* acts cell nonautonomously to repress *lim3* in dorsally projecting U MNs (Figures 1B and 7B). Inappropriate expression of *eve* and *lim3* in *dHb9* mutants is consistent with *dHb9* contributing to proper neuronal fate by suppressing the expression of key determinants of neuronal identity. These results also hint at the possibility that dHb9 regulates cell fate in a manner analogous to its vertebrate homologs.

We have characterized several cell fate changes in *dHb9* mutant embryos, and begun to pair these phenotypes with *dHb9* function in distinct neurons. However, dHb9 is expressed in approximately 30 neurons, and we have identified regulatory targets in only a handful of these cells, strongly suggesting that additional targets exist. Given the enormous complexity of the genetic regulatory network that dictates neuronal fate, the power of *Drosophila* genetics should provide an indispensable tool for identifying dHb9-interacting genes—as well as other key determinants of neuronal identity.

dHb9, lim3, islet, and the Combinatorial Code

In the vertebrate neural tube, Hb9, Lim3/4, and Isl1 are elements of a combinatorial code directing neuronal identity and axonal pathfinding (Arber et al., 1999; Sharma et al., 1998; Thaler et al., 1999). Hb9 and Lim3/4 have been shown to be expressed in all MNs exiting the neural tube ventrally, though Lim3/4 are only transiently expressed in these MNs. In the *Drosophila* CNS, functional analysis and reporter construct expression data supported roles for Lim3 and Islet in regulating the projections of ventrally projecting neurons. Islet expression was proposed to be required for the identities of ISNb and ISNd MNs, while Lim3 expression in only ISNb MNs was thought to resolve ISN neurons into ISNb and ISNd classes (Thor and Thomas, 1997; Thor et al., 1999).

Our analysis of the Lim3 protein expression pattern argues against its proposed role in distinguishing ISNb trajectories from those of ISNd. We find that Lim3 is expressed much more broadly than suggested by a *lim3* reporter gene (Thor et al., 1999). Lim3 is coexpressed with dHb9 in five of the six major motor axon branches. In addition, Lim3 but not dHB9 is expressed in the TN motor axon branch (Thor et al., 1999). Lim3 is then expressed in neurons that populate all motor axon branches. Thus, differential expression of Lim3 is insufficient to explain how neurons choose between ISNb and ISNd.

One question that then arises is why the motor axon phenotypes of *dHb9* and *lim3* mutants are specific to the ISNb nerve branch when these factors are expressed widely in MNs. It is possible that the ISNb is generally more sensitive to genetic perturbations than other motor axon branches. Consistent with this, guidance molecules with broad CNS expression patterns display motor axon phenotypes largely confined to ISNb (Desai et al., 1996; Krueger et al., 1996). Alternatively, the axonal phenotypes may be ISNb specific because dHb9 and Lim3 are expressed in a higher percentage of ISNb-projecting neurons than neurons projecting in other nerve branches. For example, eight MNs that project dorsally in the ISN are Eve positive and dHb9/Lim3 negative (Figure 3; Doe et al., 1988; Landgraf et al., 1999).

While our data argue against the simple combinatorial code proposed to regulate axon pathway choice, it is still certainly true that a neuron's fate is established largely by the combination of transcription factors it expresses. However, the fact that dHb9, Lim3, and Isl are coexpressed in a large number of neurons with different identities indicates that individual neuronal identities are not defined by the mere presence or absence of these factors. Clearly additional as yet unidentified factors are required to create the tremendous cellular diversity found in the CNS.

Additional layers of complexity also likely exist within the combinatorial code. For example, the levels and timing of expression of individual transcription factors may play important roles in directing different cellular fates. Consistent with this possibility, while dHb9 and Lim3 have largely overlapping expression patterns, their relative levels and duration of expression vary between neurons. Our data establish that these two factors act largely in parallel to establish neuronal identity. It will therefore be critical to determine whether dHb9 and Lim3 act independently on distinct targets or together as members of one transcriptional complex. In this context, it is possible that changes in the relative levels of dHb9/Lim3 would alter the composition and functional properties of these complexes. Clearly, future research that identifies additional genes with roles in neuronal fate determination and integrates their functions into the regulatory network that controls neuronal diversity will provide a more lucid picture of the genetic and molecular basis of neuronal diversity.

Crossrepressive Interactions and the Control of Neuronal Fate

Our data demonstrate that a crossinhibitory interaction between dHb9 and Eve contributes to their mutually exclusive expression patterns—Eve is expressed in dorsally projecting MNs, and dHb9 is expressed in more ventrally projecting MNs. Furthermore, functional studies demonstrate that Eve and dHb9 regulate axonal trajectories of dorsally and ventrally projecting axons, respectively (Figure 3; Landgraf et al., 1999). Together, these results suggest that the crossrepressive relationship between dHb9 and Eve helps to ensure that neurons in these two populations acquire distinct identities.

The mutual antagonism of Eve and dHb9 is similar to the relationship between pairs of HD factors whose crossrepressive interactions are central to neural tube patterning. In the vertebrate neural tube, domains of HD protein expression in distinct progenitor domains are established in response to a Shh gradient (see Jessell, 2000). Crossrepressive interactions between these HD factors then appear to refine and maintain the progenitor domains (Briscoe et al., 2000). Muhr et al. (2001) have recently shown that these proteins likely function as transcriptional repressors and may require the corepressor Groucho (Gro).

Our results suggest that Eve and dHb9 also mediate their crossrepressive interaction in a Gro-dependent manner. The ability of Eve to repress dHb9 depends on its Gro-interaction domain (Figure 6F), implicating Gro in the Eve side of this crossinhibitory interaction. In support of the idea that dHb9 acts through Gro to repress Eve, we have identified a potential Gro-interaction domain in dHb9 (Figure 1F). Clearly, the significance of this conserved domain with respect to dHb9 function must be tested in vivo. Nonetheless, these results highlight the significant mechanistic conservation of neuronal fate specification between *Drosophila* and vertebrates.

We have demonstrated that the mutually exclusive expression patterns of Eve and dHb9 arise in part through a crossinhibitory interaction between the two proteins. *dHb9* mutant embryos display several additional Eve-positive neurons, and *eve* mutants exhibit several additional dHb9-positive neurons, arguing that the Eve and dHb9 expression patterns are established largely independently and then refined by the mutually repressive interaction. In the future, it will be important to identify upstream regulators of *eve* and *dHb9* to understand the manner in which these distinct patterns of gene expression arise. Research in this area is likely to be of general relevance since in *Drosophila* and vertebrates, Hb9 and Lim3 are coexpressed in nearly identical populations of MNs (this study; Arber et al., 1999; Thaler et al., 1999). These data argue that Hb9/Lim3-positive MNs constitute an evolutionarily conserved MN population. Given this, we expect significant overlap between the upstream regulators of *dHb9*/*Lim3* in *Drosophila* and vertebrates.

dHb9 and Cell-Nonautonomous Control of CNS Cell Fate

Present models of neuronal specification in *Drosophila* suggest that cell fate is largely determined via lineage intrinsic mechanisms. In this context, our results indicating that *dHb9* acts cell nonautonomously to inhibit Lim3 expression in the U MNs uncover a novel role for intercellular signaling in the establishment of neuronal fate. During their development, U MNs are surrounded by several groups of dHb9-positive neurons (Figures 6A and 6B). One or more of these groups likely serves as the source of the dHb9-dependent signal received by the U MNs. Preliminary attempts at identifying the molecular nature of this signaling pathway indicate that the *ras, wg,* and *TGF-*β pathways are unlikely to mediate this interaction (data not shown). In the future, it will be important to identify both the cellular source as well as the molecular identity of the dHb9-dependent signal.

As noted above, subsequent to NB patterning, neuronal fate specification in the *Drosophila* CNS is thought to depend largely on cell-intrinsic factors (Goodman and Doe, 1993; Huff et al., 1989). In fact, the only well-characterized examples of intercellular signaling in this context involve the resolution of asymmetric sibling neuron fates by Notch pathway members (Spana et al., 1995; Skeath and Doe, 1998). This "lineage-intrinsic" model is based on the ability of NBs to undergo limited aspects of differentiation in culture, as well as the invariance of neuronal progeny produced within lineages. However, these observations do not exclude the possibility that stereotyped intercellular signaling plays a critical role in neuronal fate acquisition. In fact, this study indicates that intercellular signaling does in fact contribute to the consolidation of neuronal identity. As genes with increasingly subtle phenotypes are identified, we expect there will be many more examples of intercellular signaling in the *Drosophila* CNS. This theme has been borne out by work in other systems with invariant lineages such as *C. elegans* whose development was believed to be dominated by cell-intrinsic factors, but is now characterized by the presence of many well-established cell-nonautonomous interactions (Koelle and Horvitz, 1996; Sagasti et al., 2001).

Experimental Procedures

Fly Stocks

We isolated four independent *dHb9* alleles in a large-scale EMS mutagenesis screen of the third chromosome (J.B.S. and C.Q. Doe, unpublished data). In addition, we used the following fly stocks: *UAS-GAPGFP* (A. Chiba), *UAS-isl* and *lim3A-*τ*myc* (S. Thor), *elavGal4* (A. DiAntonio), *UAS-eve* (A. Brand), *Df(3L)pbl*^{NR} (R. Saint), *Df(2R)eve, eve*Δ*LFKPY*, and an *Eve-*τ*lacZ* reporter (e5tZ3R79R92-M) expressed in GMC4-2a and 1-1a and their progeny (M. Fujioka). All other stocks were obtained from the Bloomington Stock Center

Cloning of the *dHb9* Locus

We meiotically mapped *dHb9* against a *ru h th st cu sr e*^{s} *ca* third chromosome. We further mapped *dHb9* with deficiencies spanning the *ru h* interval and localized dHb9 between 66B1-2 due to its failure to complement *Df(3L)pbl*^{NR}. We screened genes in this interval for CNS expression using RNA in situ hybridization and sequenced viable candidates from homozygous mutant (dead) larvae for each *dHb9* allele, as *dHb9* mutant embryos die as first instar larvae. All four alleles result in premature stop codons: *dHb9*^{KK30} contains a C-to-T conversion at base 646; *dHb9*^{AD121} contains a C-to-T conversion at base 1003; *dHb9*^{TT219} contains a C-to-T conversion at base 1435; and *dHb9*^{JJ154} contains a G-to-A conversion at base 1589.

dHb9 cDNA and UAS-dHb9

We isolated a full-length *dHb9* cDNA via RT-PCR from RNA prepared from a 0–20 hr collection of Oregon R embryos. *polyA* RNA was prepared using the RNeasy midi kit and oligotex beads (Qiagen) and converted into cDNA using superscript II reverse transcriptase (Gibco BRL). *dHb9* cDNA was generated using primers that amplify from the predicted start to the predicted stop codon. We cloned and sequenced the 1575 bp product, which matched the Celera prediction at the protein level. To create *UAS-dHb9*, we inserted the *dHb9* cDNA into the Not1 site of pUAST (Brand and Perrimon, 1993) and created germline transformants following standard methods.

Antibody Production, Immunofluorescent, and Immunohistochemical Studies

Amino acids 204–525 of dHb9, amino acids 144–430 of Lim3, and amino acids 1–213 of Isl were cloned into pET (Novagen) for protein expression and purification. These antigens were used to immunize rabbits and guinea pigs (anti-dHb9), guinea pigs (anti-Lim3), and rats (anti-Isl) at Pocono Rabbit Farm. The Lim3 and Isl antibodies are specific as they do not recognize antigen on embryos homozygous mutant for deficiencies of the respective loci: *Df(2L) TW130 (lim3)* and *Df(2L)OD15 (Isl)*.

The following primary antibodies were used: rabbit anti-GFP (P. Levin), rabbit anti-Eve (M. Frasch), mouse anti-Eve (N. Patel), mouse anti-Myc (Sigma), rabbit anti-β-gal (ICN), mouse anti-β-gal (Promega), rabbit anti-PH3 (Upstate Biotech), and mouse monoclonal 1D4 (anti-FasII) and mouse monoclonal BP102 (both from C. Goodman). We used the Vector ABC kit for immunohistochemistry and Alexa-488 and Alexa-568 with appropriate species specificity for immunofluorescence (Molecular Probes).

***dHb9{LacZ}* and *dHb9{Gal4 }* Enhancer Trap Lines**

We generated five P{LacZ}*dHb9* alleles in a standard local P element transposition screen, using *pbl*^{P008320} as a donor P element (Zhang and Spradling, 1993). Of 2034 F2 males bearing putative new insertions, five were *dHb9* P element alleles, and one of these was an enhancer trap of the *dHb9* locus. We used this allele to create a *dHb9*^{Gal4} enhancer trap in a strategy modified from Sepp and Auld (1999). Briefly, we crossed *P{Gal4w*$^{+}$*}/FM7; dHb9P{LacZ}/TM3* females to transposase-bearing males. *P{Gal4w*$^{+}$*}/w; dHb9*$^{P[LacZ]}$*/TM3 Delta2-3* F1 virgins were collected and crossed to UAS-GFP males. We screened larvae from this cross for CNS expression of GFP and identified 15 larvae with CNS GFP expression. Two produced viable offspring that expressed Gal4 in the correct pattern.

Acknowledgments

We thank A. Brand, A. Chiba, A. DiAntonio, M. Fujioka, C. Goodman, R. Saint, S. Thor, and the Bloomington Stock Center for reagents; and K. O'Connor-Giles and A. DiAntonio for critical reading of the manuscript. We are also indebted to C. Kadavi and Y. Zhu for invaluable technical assistance. We are particularly grateful to an anonymous reviewer for suggestions that greatly improved this manuscript. This work was supported by an NRSA NIH postdoctoral fellowship (H.T.B.) and by an NINDS grant (R01-NS-36570) (J.B.S.).

Received: August 14, 2001
Revised: May 7, 2002

References

Appel, B., Korzh, V., Glasgow, E., Thor, S., Edlund, T., David, I.B., and Eisen, J.S. (1995). Motoneuron fate specification revealed by patterned LIM homeobox gene expression in embryonic zebrafish. Development *121*, 4117–4125.

Arber, S., Han, B., Mendelsohn, M., Smith, M., Jessell, T.M., and Sockanathan, S. (1999). Requirement for the homeobox gene *Hb9* in the consolidation of motor neuron identity. Neuron *23*, 659–674.

Bossing, T., Udolph, G., Doe, C.Q., and Technau, G.M. (1996). The embryonic CNS lineages of *Drosophila melanogaster* I. Neuroblast lineages derived from the ventral half of the neuroectoderm. Dev. Biol. *179*, 41–64.

Brand, A.H., and Perrimon, N. (1993). Targeted gene expression as a means of altering cell fates and generating dominant phenotypes. Development *118*, 401–415.

Briscoe, J., Pierani, A., Jessell, T.M., and Ericson, J. (2000). A homeodomain protein code specifies progenitor cell identity and neuronal fate in the ventral neural tube. Cell *101*, 435–445.

Desai, C.J., Gindhart, J.J., Goldstein, L.S.B., and Zinn, K. (1996). Receptor tyrosine phosphatases are required for motor axon guidance in the *Drosophila* embryo. Cell *84*, 599–609.

Doe, C.Q., Smouse, D., and Goodman, C.S. (1988). Control of neuronal fate by the Drosophila segmentation gene *even-skipped*. Nature *333*, 376–378.

Fujioka, M., Emi-Sarker, Y., Yusibova, G.L., Goto, T., and Jaynes, J.B. (1999). Analysis of an even-skipped rescue transgene reveals both composite and discrete neuronal and early blastoderm enhancers, and multi-stripe positioning by gap gene repressor gradients. Development *126*, 2527–2538.

Goodman, C.S., and Doe, C.Q. (1993). Embryonic development of the *Drosophila* central nervous system. In The Development of *Drosophila melanogaster,* M. Bate and A. Martinez Arias, eds. (Cold Spring Harbor, NY: Cold Spring Harbor Laboratory Press), pp. 1131–1206.

Huff, R., Furst, A., and Mahowald, A.P. (1989). *Drosophila* embryonic neuroblasts in culture: autonomous differentiation of specific neurotransmitters. Dev. Biol. *134*, 146–157.

Jessell, T.M. (2000). Neuronal specification in the spinal cord: inductive signals and transcriptional codes. Nat. Rev. Genet. *1*, 20–29.

Jiménez, G., Paroush, Z., and Ish-Horowicz, D. (1997). Groucho acts as corepressor for a subset of negative regulators, including Hairy and Engrailed. Genes Dev. *11*, 3072–3082.

Kobayashi, M., Goldstein, R.E., Fujioka, M., Paroush, Z., and Jaynes, J.B. (2001). Groucho augments the repression of multiple Even skipped target genes in establishing parasegment boundaries. Development *128*, 1805–1815.

Koelle, M.R., and Horvitz, R. (1996). Egl-10 regulates G protein signaling in the *C. elegans* nervous system and shares a conserved domain with many mammalian proteins. Cell *84*, 115–125.

Krueger, N.X., Van Vactor, D., Wan, H.I., Gelbart, W.M., Goodman, C.S., and Saito, H. (1996). The transmembrane tyrosine phosphatase DLAR controls motor axon guidance in *Drosophila*. Cell *84*, 611–622.

Landgraf, M., Bossing, T., Technau, G.M., and Bate, M. (1997). The origin, location, and projections of the embryonic abdominal motorneurons of *Drosophila*. J. Neurosci. *17*, 9642–9655.

Landgraf, M., Roy, S., Prokop, A., VijayRaghavan, K., and Bate, M. (1999). *even-skipped* determines the dorsal growth of motor axons in *Drosophila*. Neuron *22*, 43–52.

Lundell, M., and Hirsch, J. (1994). Temporal and spatial development of serotonin and dopamine neurons in the *Drosophila* CNS. Dev. Biol. *165*, 385–396.

Moran-Rivard, L., Kagawa, T., Saueressig, H., Gross, M.K., Burrill, J., and Goulding, M. (2001). Evx1 Is a postmitotic determinant of VO interneuron identity in the spinal Cord. Neuron *29*, 385–399.

Muhr, J., Andersson, E., Persson, M., Jessell, T.M., and Ericson, J. (2001). Groucho-mediated transcriptional repression establishes progenitor cell pattern and neuronal fate in the ventral neural tube. Cell *104*, 861–873.

Patel, N.H., Schafer, B., Goodman, C.S., and Holmgren, R. (1989). The role of segment polarity genes during *Drosophila* neurogenesis. Genes Dev. *3*, 890–904.

Sagasti, A., Hisamoto, N., Hyodo, J., Tanaka-Hino, M., Matsumoto, K., and Bargmann, C.I. (2001). The CaMKII UNC-43 activates the MAPKKK Nsy-1 to execute a lateral signaling decision required for asymmetric olfactory neuron fates. Cell *105*, 221–232.

Saha, M.S., Miles, R.R., and Grainger, R.M. (1997). Dorsal-ventral patterning during neural induction in *Xenopus*: assessment of spinal cord regionalization with *xHb9*, a marker for the motor neuron region. Dev. Biol. *187*, 209–223.

Schmid, A., Chiba, A., and Doe, C.Q. (1999). Clonal analysis of *Drosophila* embryonic neuroblasts: neural cell types, axon projections and muscle targets. Development *126*, 4653–4689.

Sepp, K.J., and Auld, V.J. (1999). Conversion of *lacZ* enhancer trap lines to GAL4 lines using targeted transposition in *Drosophila melanogaster*. Genetics *151*, 1093–1101.

Sharma, K., Sheng, H.Z., Lettieri, K., Li, H., Karavanov, A., Potter, S., Westphal, H., and Pfaff, S.L. (1998). LIM homeodomain factors Lhx3 and Lhx4 assign subtype identities for motor neurons. Cell *95*, 817–828.

Skeath, J.B., and Doe, C.Q. (1998). Sanpodo and Notch act in opposition to Numb to distinguish sibling neuron fates in the *Drosophila* CNS. Development *125*, 1857–1865.

Spana, E.P., Kopczynski, C., Goodman, C.S., and Doe, C.Q. (1995). Asymmetric localization of numb autonomously determines sibling neuron identity in the *Drosophila* CNS. Development *121*, 3489–3494.

Tanabe, Y., William, C., and Jessell, T.M. (1998). Specification of motor neuron identity by the MNR2 homeodomain protein. Cell *95*, 67–80.

Thaler, J., Harrison, K., Sharma, K., Lettieri, K., Kehrl, J., and Pfaff, S.L. (1999). Active suppression of interneuron programs within developing motor neurons revealed by analysis of homeodomain factor Hb9. Neuron *23*, 675–687.

Thor, S., and Thomas, J.B. (1997). The Drosophila *islet* gene governs axon pathfinding and neurotransmitter identity. Neuron *18*, 397–409.

Thor, S., Andersson, S.G., Tomlinson, A., and Thomas, J.B. (1999). A LIM-homeodomain combinatorial code for motor-neuron pathway selection. Nature *397*, 76–80.

Tsuchida, T., Ensini, M., Morton, S.B., Morton, S.B., Baldassare, M., Edlund, T., Jessell, T.M., and Pfaff, S.L. (1994). Topographic organization of embryonic motor neurons defined by expression of LIM homeobox genes. Cell *79*, 957–970.

Van Vactor, D., Sink, H., Fambrough, D., Tsoo, R., and Goodman, C.S. (1993). Genes that control neuromuscular specificity in *Drosophila*. Cell *73*, 1137–1153.

Zhang, P., and Spradling, A.C. (1993). Efficient and dispersed local P element transposition from *Drosophila* females. Genetics *133*, 361–373.